Theoretical investigation of the potential energy surface for the NH2+NO reaction via density functional theory and ab initio molecular electronic structure theory

Eric W.-G. Diau and Sean C. Smith

Citation: J. Chem. Phys. **106**, 9236 (1997); doi: 10.1063/1.474025
View online: http://dx.doi.org/10.1063/1.474025
View Table of Contents: http://jcp.aip.org/resource/1/JCPSA6/v106/i22
Published by the American Institute of Physics.

Theoretical investigation of the potential energy surface for the NH_2+NO reaction via density functional theory and *ab initio* molecular electronic structure theory

Eric W.-G. Diau and Sean C. Smith
Department of Chemistry, University of Queensland, Brisbane, Qld 4072, Australia

(Received 1 August 1996; accepted 14 February 1997)

The potential energy surface of the NH_2+NO reaction, which involves nine intermediates (1–9) as well as twenty-three possible transition states ($a-w$), has been fully characterized at the B3LYP/cc-pVQZ//B3LYP/6-311G(d,p)+ZPE[B3LYP/6-311G(d,p)] and modified Gaussian-2 (G2M) levels of theory. The reaction is shown to have three different groups of products (HN_2+OH, N_2O+H_2, and N_2+H_2O denoted as **A**, **B**, and **C**, respectively) and a very complicated reaction mechanism. The first reaction path is initiated by the N–N bond association of the reactants to form an intermediate H_2NNO, **1**, which then undergoes a 1,3-H migration to yield an isomer pair HNNOH (**2,3**) (separated by a low energy torsional barrier) which can then proceed along three different paths. Because of the essential role it would play kinetically, the enthalpy of the $NH_2+NO\rightarrow HN_2+OH$ reaction has been further investigated using various levels of theory. The best theoretical results of this study predicted it to be 0.9 and 2.4 kcal mol^{-1} at the B3LYP and CCSD(T) levels, respectively, using a relatively large basis set (AUG-cc-pVQZ) based on the geometry optimized at the B3LYP/6-311G(d,p) level of theory. It has been found that TS g(**4→B**) is expected to be the rate-determining transition state responsible for the $NH_2+NO\rightarrow N_2O+H_2$ reaction. TS g lies above the reactants by only 2.6 kcal mol^{-1} according to the G2M prediction. On the other hand, TS h(**3→7**) is a new transition state discovered in this work which may allow some kinetic contribution from the $NH_2+NO\rightarrow N_2+H_2O$ reaction under high temperature conditions due to its relatively low energy as well as its loose transition state property. A modified G2 additivity scheme based on the G2(DD) approach has been shown to be necessary for better predicting the energetics for TS h, which gives a value of 2.3 kcal mol^{-1} in energy with respect to the reactants. Generally, the cost-effective B3LYP method is found to give very good predictions for the optimized geometries and vibrational frequencies of various species in the system if compare them with those optimized at the QCISD/6-311G(d,p) and 12-in-11 CASSCF/cc-pVDZ levels of theory. Furthermore, it is noticeable in this study that most of the relative energies calculated via the B3LYP method are more close to the G2M results than those predicted at the PMP4 and CCSD(T) levels using the same 6-311G(d,p) basis set. © *1997 American Institute of Physics.* [S0021-9606(97)01719-4]

I. INTRODUCTION

The reaction of NH_2 with NO is of considerable interest due to its essential role in the thermal $DeNO_x$ process.[1–5] Numerous investigations for the reaction system have been carried out via direct kinetic measurements,[6–12] high temperature kinetic modeling,[4,13–17] *ab initio*/molecular orbital (MO) theory,[18–23] and Rice–Ramsperger–Kassel–Marcus (RRKM) calculations.[11,19,24,25] In view of the thermochemistry for the system, three exit channels may be involved in the reaction mechanism according to their reaction enthalpies,

$$NH_2+NO\xrightarrow{k_1}HN_2+OH \quad (1)$$

$$\xrightarrow{k_2}N_2O+H_2 \quad (2)$$

$$\xrightarrow{k_3}N_2+H_2O, \quad (3)$$

where reaction (1) is thermoneutral and reactions (2) and (3) exothermic by 47.2 and 124.8 kcal mol^{-1}, respectively.[26] Recent kinetic measurement[13] has shown that the contribution from reaction (2) was negligible in this system with temperature up to 1060 K. However, reaction (2) has been observed directly by a shock tube study in the temperature range between 1680 and 2850 K.[13] On the other hand, a very high barrier (32 kcal mol^{-1}) was predicted for this reaction by bond additivity corrections with fourth-order Møller–Plesset perturbation theory (BAC-MP4),[20] which apparently ruled out the possibility of the NH_2+NO reaction proceeding through channel (2).

The product branching ratio of reaction (1), $\alpha=k_1/(k_1+k_2+k_3)$, is a key factor in the kinetic modeling of this system under combustion conditions due to the fact that reaction (1) is a chain branching step.[3–5] For this reason, it has been the focus of much attention experimentally[7–9,12,14–17] in recent years. However, the comparison between the temperature dependence of α measured from direct laser kinetic studies and that measured indirectly from high temperature flame modeling still remains controversial. Only a limited number of theoretical calculations[11,25]

 0021-9606/97/106(22)/9236/16/$10.00

of α have been performed because of the complexity of the multichannel reaction mechanism, with several barrierless bond-association steps involved. Recently, we have calculated the temperature dependence of α between 300 and 3000 K using a combined Microcanonical Variational Transition State Theory (μVTST)/RRKM theory treatment, abbreviated henceforth as μVRRKM. This calculation was based on the potential energy surface (PES) calculated by Walch[22] at the complete active space self-consistent-field (CASSCF)/internally contracted configuration interaction (ICCI) level of theory with Morse model potentials for the minimum energy pathways (MEPs) of the barrierless channels.[25] The results for α predicted by μVRRKM theory agree well with the room temperature data as well as those obtained from high temperature kinetic modeling, however, the agreement with the direct laser kinetic studies between 300 and 1000 K was not very good. It has also been pointed out[25] that further characterization of the temperature dependence of α via μVRRKM theory requires more complete parameters from high-level *ab initio* calculations for the PES and MEPs of this system.

In this paper, the first part of an extensive investigation of the NH_2+NO reaction, we focus on the determination of the stationary points associated with a complete PES for the reaction between NH_2 and NO, using several advanced techniques. After a brief introduction to the computational procedures, we give optimized geometries, normal vibrational frequencies, and energies for a total of nine intermediates as well as twenty-three possible transition states which connect intermediates or lead to the product channels. A new reaction path will be presented to elucidate the possibility of the NH_2+NO reaction proceeding through channel (2) under shock tube conditions. This enables a more complete formulation of the reaction mechanism of this system for the purpose of implementation of accurate μVRRKM calculations.

II. COMPUTATIONAL PROCEDURES

The geometries of the reactants, products, intermediates, and transition states have been optimized with Density Functional Theory (DFT) at the B3LYP/6-311G(d,p) level, where B3LYP stands for Becke's three-parameter nonlocal exchange functional[27] with the nonlocal correlation of Lee, Yang, and Parr,[28] and 6-311G(d,p) is a notation for split-valence triple-zeta basis sets introduced by Pople and co-workers.[29] Note that the spin-restricted and spin-unrestricted wave functions were used for the close shell species (all intermediates and transition states) and the open shell species (reactants and radical products), respectively. For comparison, geometry optimizations for some transition states have also been carried out using the B3LYP/6-311+$G(d,p)$,[27(a)] MP2/6-311G(d,p),[29] MP2/6-311 + $G(d,p)$,[29] and QCISD/6-311G(d,p) (Ref. 30) methods.

Vibrational frequencies have been calculated at the B3LYP/6-311G(d,p) level for characterization of the nature of the stationary points, determination of the zero-point energy (ZPE) corrections, prediction of vibrational spectra, and/or evaluation of the rate coefficients for the system. All the stationary points have been positively identified as local minima or transition states. In order to confirm that the transition states connect designated intermediates, Intrinsic Reaction Coordinate (IRC) calculations[31] have also been performed at the B3LYP/6-311G(d,p) level of theory.

Based on the B3LYP/6-311G(d,p) optimized geometries, the relative energies were further calculated at the spin-projected unrestricted (P) MP4/6-311G(d,p), CCSD(T)/6-311G(d,p), and B3LYP/cc-pVQZ levels of theory, where cc-pVQZ is an abbreviation for Dunning's correlation consistent quadruple-zeta basis sets with valence polarization functions.[32] In order to obtain more reliable energies, the Gaussian-2 (G2) type methodology[33–39] has also been implemented in this study. The conventional G2 method[33] uses a series of *ab initio* calculations with various basis sets to approximate a QCISD(T)/6-311+G(3df,2p)//MP2/6-31G(d) calculation with an additional ''higher level correction'' (HLC) based on the number of paired and unpaired electrons. However, significant effort has been made to further improve the G2 theory with the G2Q,[34] G2(PU),[35] G2M,[36,37] G2(MP2,SVP),[38] or the G2(DD) (Ref. 39) calculation for different purposes. For the present energy calculations we employed the G2M(CC1) method developed by Mebel *et al.*[37] for all species. The additivity scheme of G2M(CC1) aims to achieve a composite energy calculation at the CCSD(T)/6-311+G(3df,2p)//B3LYP/6-311G(d,p) level. Other accurate methods based on the G2Q, G2(PU), or the G2(DD) approach have also been utilized on QCISD/6-311G(d,p) optimized geometries with HLC and ZPE corrections for a few specific transition states for comparison.

The enthalpy of reaction (1), $\Delta H^0_{(1)}$, has been shown in our previous μVRRKM study[25] to be vital for the accurate modeling of the system. For this reason, $\Delta H^0_{(1)}$ has been examined with various levels of theory in addition to the aforementioned ones, such as BLYP/6-311G(d,p), B3LYP/AUG-cc-pVQZ, PMP4/AUG-cc-pVQZ, QCISD(T)/6-311++G(2df,p), CCSD(T)/AUG-cc-pVQZ, and the complete basis set-quadratic configuration interaction/atomic pair natural orbital (CBS-QCI/APNO) method.[40] All calculations were performed using the GAUSSIAN 94 program.[41]

III. RESULTS AND DISCUSSION

The reaction of the NH_2 and NO radicals is initiated by an association step to form a stable intermediate, H_2NNO, **1**, without any pronounced energy barrier.[42] Another possibility, that of hydrogen abstraction, leads to the production of NH and HNO with endothermicity by 46.8 kcal mol^{-1}.[26] Therefore, the following discussion will concentrate on the possible isomerization/dissociation and subsequent steps after **1** has been formed.

The B3LYP/6-311G(d,p) optimized geometries of reactants, products, and intermediates of the reaction are shown in Fig. 1, and those of the transition states shown in Fig. 2. The relative energies of all species calculated at various levels of theory are presented in Table I, and theB3LYP/

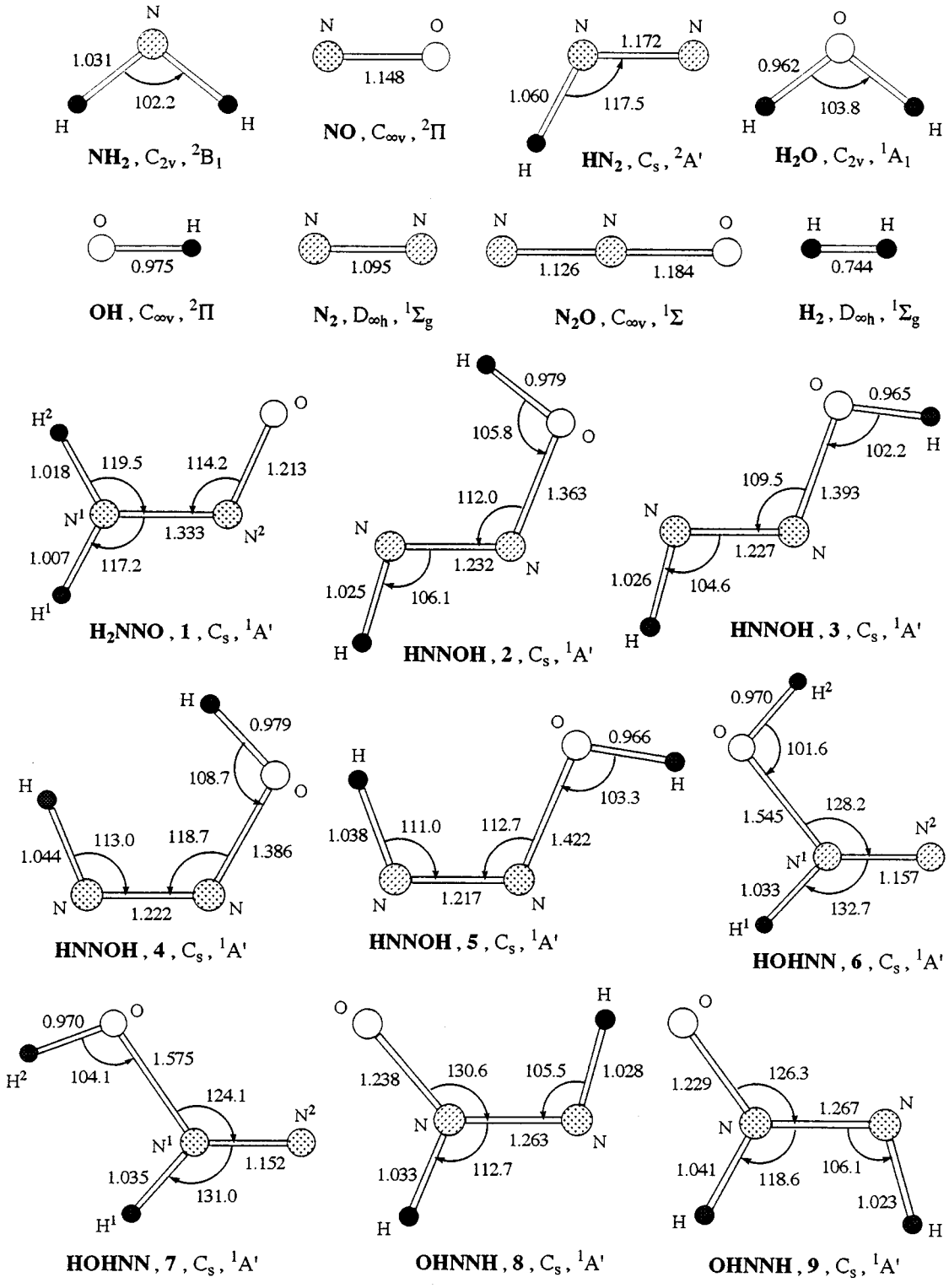

FIG. 1. B3LYP/6-311G(d,p) optimized geometries (in Å and deg) of the reactants, products, and intermediates involved in the NH_2+NO reaction.

6-311G(d,p) normal vibrational frequencies for intermediates and transition states presented in Table II. Figure 3 shows the potential energy profile of the system at the G2M(CC1) level of theory with the important intermediates (**1**–**7**) and transition states (a–n) which may be involved in the mechanism of the reactions (1), (2), or (3). It is indicated that a 1,3-H migration process (saddle point located at TS a) connects the reaction path between the intermediates **1** and **2**, and a low energy torsional barrier is involved between **2** and **3**. The isomer pair, HNNOH (**2**,**3**), can then proceed with three different paths; (i) directly dissociates into radical product group **A** (HN_2+OH) with no barrier with respect to

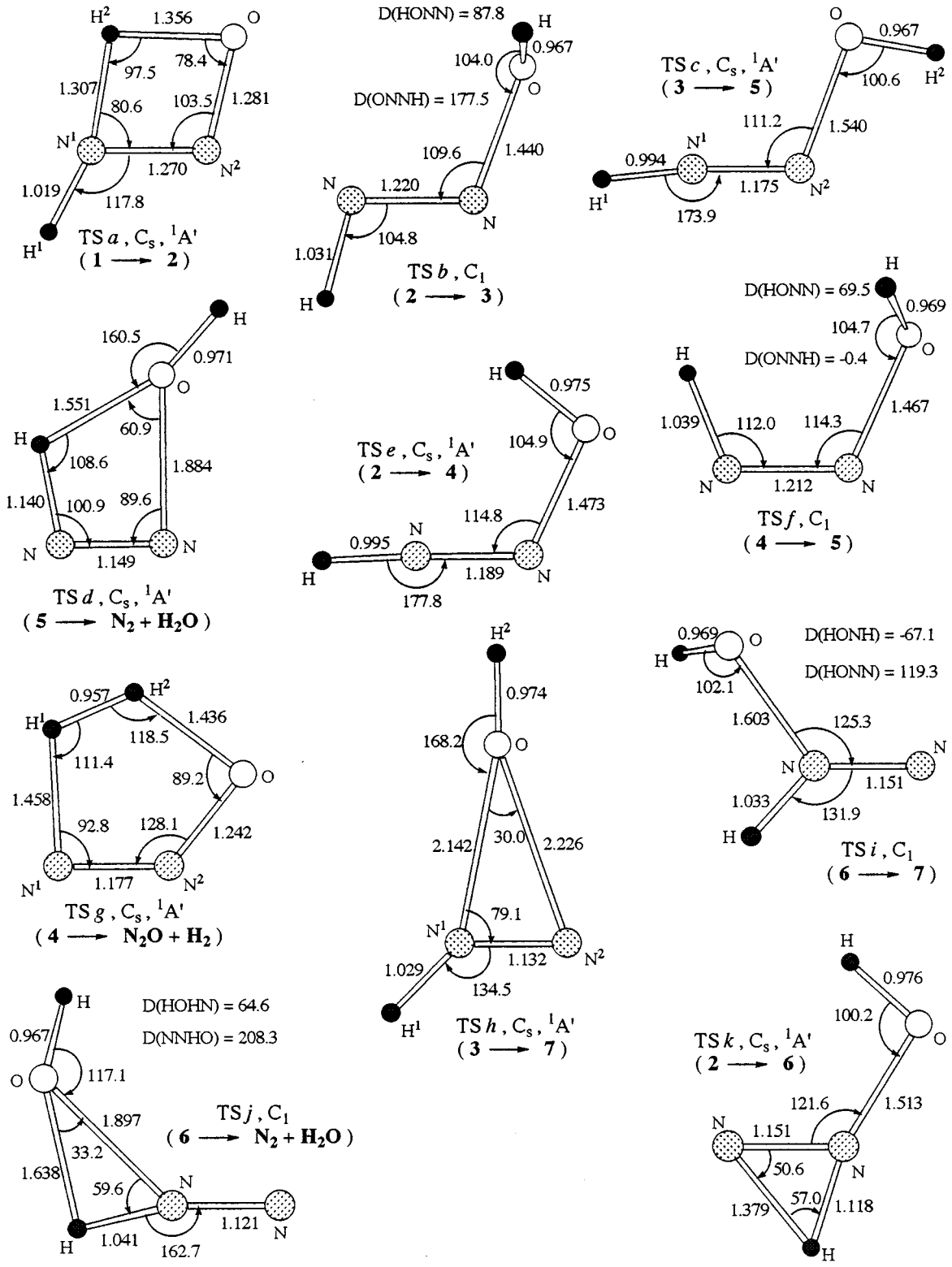

FIG. 2. B3LYP/6-311G(d,p) optimized geometries (in Å and deg) of the possible transition states involved in the NH_2+NO reaction.

HN_2+OH involved; (ii) undergoes a *cis–trans* isomerization to form another isomer pair HNNOH (**4**,**5**) through the corresponding transition state (TS *c* or TS *e*); (iii) takes place a 1,2-OH shift to form the other isomer pair HOHNN (**6**,**7**) via a loose transition state, TS *h*. The HNNOH (**4**,**5**) generated from step (ii) can either directly dissociate to form product group **A**, produce product group **B** (N_2O+H_2) from **4** through a five-member-ring transition state, TS *g*, or ultimately lead to product group **C** (N_2+H_2O) from **5** through a four-member-ring transition state, TS *d*. The HOHNN (**6**,**7**)

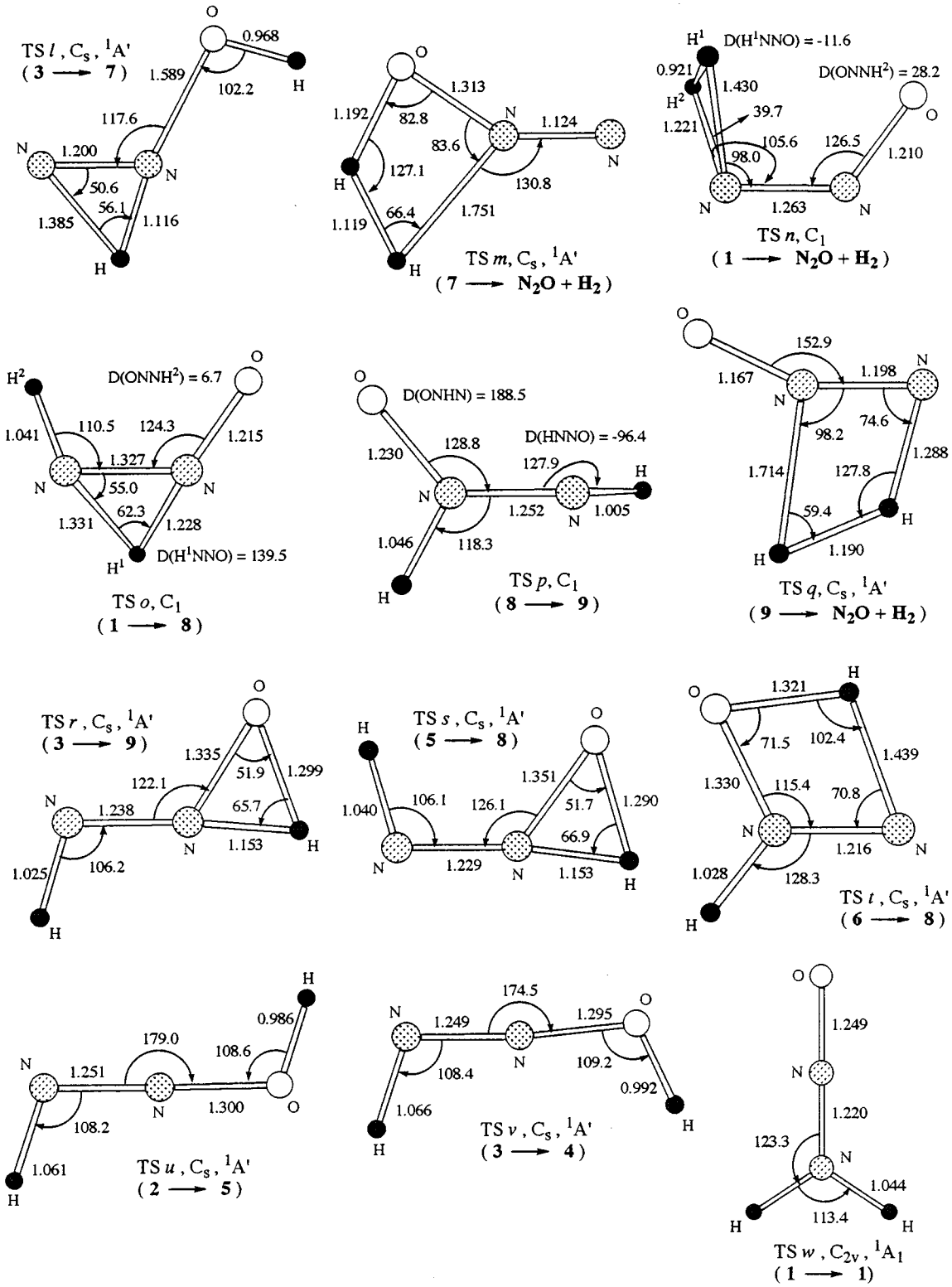

FIG. 2. (*Continued.*)

can also directly dissociate to form product group **A**, but most likely it would instantly lead to product group **C** from **6** through a nonplanar transition state (TS *j*) with a very low energy barrier involved.

A. Reaction enthalpies $\Delta H^0_{(1)}$, $\Delta H^0_{(2)}$, and $\Delta H^0_{(3)}$ at 0 K

The enthalpies of both reactions (2) and (3) are good indicators to judge the accuracy of calculations since accu-

TABLE I. Relative energies of reactants, products, intermediates, and transition states for the NH_2+NO reaction at various levels of theory.[a]

Species	Present work										CASSCF/ICCl[k]	
	ZPE[b]	B3LYP[c]	B3LYP[d]	PMP4[e]	CCSD(T)[e]	G2M(CCl)[f]	GVB-Cl[g]	BAC-MP4[h]	MP4SDQ[i]	CASSCF /SCF-Cl[j]	Ref. 1	Ref. 2
NH_2+NO[l]	14.7	0.0	0.0	0.0	0.0	0.0	0.0	0.0	0.0	0.0	0.0	0.0
HN_2+OH, **A**	13.5	1.8	1.2	6.7	3.7	3.6		2.4	6.1	3.0	0.7	
N_2O+H_2, **B**[m]	13.3	− 45.9	− 45.4	− 49.4	− 42.5	− 48.2		− 48.4		− 31.9	− 47.2[o]	− 41.3
N_2+H_2O, **C**[n]	16.8	−111.8	−114.7	−117.7	−118.1	−124.3	−123.7[o]	−124.0	−113.0	−120.0	−124.0	−118.1
H_2NNO, **1**	20.3	− 45.7	− 44.2	− 38.3	− 38.5	− 46.7	− 29.0	− 48.1	− 36.5	− 34.7	− 44.0	− 38.1[o]
HNNOH, **2**	21.0	− 42.9	− 42.7	− 37.8	− 39.3	− 46.6	− 31.3	− 47.5	− 35.6	− 36.7	− 45.7	− 39.8
HNNOH, **3**	21.1	− 41.2	− 41.6	− 36.0	− 37.7	− 46.0	− 30.4	− 45.5	− 33.7	− 35.9	− 44.5	− 38.6
HNNOH, **4**	20.2	− 36.5	− 36.5	− 31.4	− 32.6	− 40.2	− 23.2	− 41.1	− 28.6	− 29.9		
HNNOH, **5**	20.6	− 42.9	− 42.4	− 37.6	− 39.1	− 46.3	− 31.7	− 47.2	− 35.5	− 36.3	− 45.5	− 39.6
HOHNN, **6**	20.0	− 25.6	− 25.7	− 16.7	− 18.5	− 28.0	− 7.4	− 24.4				
HOHNN, **7**	19.4	− 19.9	− 21.1	− 10.4	− 12.6	− 23.3	1.5					
OHNNH, **8**	21.9	− 35.3	− 35.1	− 29.7	− 28.5	− 37.8	− 15.3	− 39.4				
OHNNH, **9**	21.6	− 29.1	− 30.3	− 23.0	− 22.0	− 32.8	− 5.6	− 32.3				
TS *a*, **1→2**	17.6	− 13.6	− 12.6	− 8.7	− 7.6	− 14.8		− 19.7	− 2.4	− 0.1	− 14.4	− 8.5
TS *b*, **2→3**	19.9	− 32.4	− 33.0	− 27.8	− 29.8	− 37.8			− 25.6	− 27.9	− 35.7[p]	− 29.8[p]
TS *c*, **3→5**	18.4	− 8.6	− 9.7	1.3	0.6	−10.9(−10.3)		− 7.0	6.9	3.4	− 7.4	− 1.5
TS *d*, **5→C**	16.5	− 20.0	− 19.9	− 16.3	− 15.4	− 24.9		− 25.2	− 7.5	− 8.8	− 21.9	− 16.1
TS *e*, **2→4**	18.2	− 6.4	− 7.1	3.2	2.4	− 8.1			8.3	5.3		
TS *f*, **4→5**	19.4	− 32.7	− 33.0	− 27.9	− 29.5	− 37.4			− 27.2	− 27.4		
TS *g*, **4→B**	15.2	2.4	3.6	2.4	8.3	2.6				19.9		
TS *h*, **3→7**	17.3	15.5	11.5	16.8	16.8	0.8(4.5)		65.0				
TS *i*, **6→7**	19.0	− 19.7	− 21.0	− 11.0	− 12.9	− 23.4						
TS *j*, **6→C**	16.8	− 14.7	− 17.2	− 10.0	− 6.1	− 20.4		− 4.3[p]				
TS *k*, **2→6**	15.8	22.3	21.8	25.7	26.3	16.6						
TS *l*, **3→7**	15.9	21.7	20.5	24.2	25.6	14.8		27.9				
TS *m*, **7→B**	13.6	35.7	35.9	40.6	42.7	35.9						
TS *n*, **1→B**	13.8	25.8	25.9	38.5	37.6	28.8		32.2				
TS *o*, **1→3**	17.0	14.5	15.0	19.7	21.5	12.8		9.5				
TS *p*, **8→9**	19.8	1.6	0.1	10.6	12.0	− 0.3						
TS *q*, **9→B**	13.5	63.7	64.3	65.5	72.8	66.2						
TS *r*, **3→9**	17.3	13.9	12.7	18.8	21.0	10.0						
TS *s*, **5→8**	17.2	11.6	11.3	16.4	18.5	8.6		4.5				
TS *t*, **6→8**	18.1	9.7	9.8	16.3	16.0	7.1						
TS *u*, **2→5**	18.5	45.3	45.8	58.3	55.8	47.0		48.0				
TS *v*, **3→4**	18.2	45.9	46.0	59.3	56.5	47.4						
TS *w*, **1→1**	18.7	30.2	31.4	48.0	46.4	36.9						

[a]All energies are in units of kcal mol^{-1} including zero-point energy (ZPE) corrections.
[b]Zero-point energy corrections were calculated at the B3LYP/6-311G(d,p) level of theory.
[c]Geometries were optimized at the B3LYP level of theory with the 6-311G(d,p) basis set.
[d]Single point energy calculations with the cc-pVQZ basis set on the optimized geometries.
[e]Single point energy calculations with the 6-311G(d,p) basis set on the optimized geometries.
[f]Refer to Table III for more detailed G2M calculations of several selected species. The values in parentheses were obtained from a further energy correction for the $\Delta E(+)$ using the CCSD(T) instead of PMP4 method, see text and Ref. 63 for more details about this correction.
[g]Reference 18, with ZPE corrections estimated from model compounds.
[h]Reference 20.
[i]Reference 21, with ZPE[HF/6-31G(d)] scaled by 0.89.
[j]Reference 23, with ZPE corrections calculated at the 12-in-11 CASSCF/cc-pVDZ level of theory. Note that the energies were computed at the HF reference Cl level with a modified cc-pVTZ basis set excluding f function.
[k]Reference 22. The energies shown in the Ref. 1 column were computed with respect to H_2+N_2O and the NH_2+NO asymptote was positioned from experiment, whereas those of the Ref. 2 column were directly computed with respect to NH_2+NO.
[l]The total energies of the NH_2+NO system are represented in the following: B3LYP/6-311G(d,p): −185.821 80, B3LYP/cc-pVQZ: −185.860 30, PMP4/6-311G(d,p): −185.400 28, CCSD(T)/6-311G(d,p): −185.394 59, G2M(CCl): −185.535 32, where the values are in units of hartree and all without ZPE corrections except for G2M.
[m]The JANAF experimental value for $[\Delta H_f^0(N_2O+H_2)-\Delta H_f^0(NH_2+NO)]$ at 0 K is −47.2 kcal mol^{-1}.
[n]The JANAF experimental value for $[\Delta H_f^0(N_2+H_2O)-\Delta H_f^0(NH_2+NO)]$ at 0 K is −124.8 kcal mol^{-1}.
[o]The reference value to be based on for locating the relative energies of the other species in the same column.
[p]Estimated values

rate experimental values are available in the literature.[26] The G2M results listed in Table I demonstrate the excellent agreement with those of experiments with uncertainties within 1 kcal mol^{-1} for both reactions. $\Delta H^0_{(2)}$ is overestimated by 1.8 kcal mol^{-1} when calculated at the B3LYP/cc-pVQZ+ZPE level of theory, however, $\Delta H^{(0)}_{(3)}$ is overestimated by about 10 kcal mol^{-1} at the same level of theory. The DFT methods have been widely recognized as good

TABLE II. B3LYP/6-311G(d,p) normal vibrational frequencies (cm^{-1}) for intermediates and transition states of the reaction of NH_2 with NO.

Species	ω_1[a]	ω_2	ω_3	ω_4	ω_5	ω_6	ω_7	ω_8	ω_9
1	190	632	723	1093	1223	1580	1609	3455	3697
2	673	677	950	956	1369	1446	1641	3415	3565
3	516	668	908	970	1334	1451	1685	3401	3810
4	521	661	882	964	1290	1416	1676	3135	3551
5	481	622	818	1019	1295	1399	1724	3230	3796
6	434	453	717	838	1194	1441	1912	3245	3742
7	171	454	661	795	1197	1401	1953	3186	3726
8	689	905	1107	1267	1451	1547	1641	3305	3400
9	734	824	1024	1263	1447	1527	1704	3151	3436
a	1893*i*	584	954	1175	1219	1374	1464	2072	3493
b	587*i*	665	822	947	1280	1415	1667	3341	3775
c	1250*i*	422	476	503	674	1220	1878	3784	3877
d	1112*i*	118	539	802	1018	1111	1968	2227	3739
e	1304*i*	338	497	579	728	1272	1803	3638	3862
f	484*i*	614	749	971	1246	1366	1705	3201	3750
g	1502*i*	769	776	1118	1220	1297	1471	1898	2066
h	533*i*	394	426	568	728	898	2103	3315	3680
i	230*i*	435	680	792	1118	1330	1945	3231	3750
j	1238*i*	260	393	516	670	853	2138	3145	3788
k	1961*i*	70	441	451	642	1252	1740	2848	3637
l	1869*i*	139	373	463	576	1128	1792	2859	3778
m	2282*i*	489	545	714	1030	1128	1491	1917	2212
n	1616*i*	279	547	900	1134	1194	1323	1643	2664
o	1957*i*	546	686	975	1279	1355	1582	2222	3219
p	1352*i*	731	779	1029	1363	1547	1626	3072	3680
q	3398*i*	496	620	772	1035	1272	1406	1802	2040
r	2038*i*	431	648	881	1118	1443	1554	2631	3417
s	2032*i*	431	598	971	1100	1429	1599	2647	3231
t	1993*i*	883	915	1107	1229	1345	1678	2088	3384
u	1173*i*	339	923	928	1326	1538	1796	2801	3281
v	1164*i*	348	923	925	1364	1482	1811	2729	3158
w	1001*i*	455	721	1049	1251	1763	1929	2897	3005

[a]The symbol *i* represents an imaginary number.

tools for determinations of the equilibrium geometry and vibrational frequencies.[36,37,43–50] In general, the accuracy for energy calculated via the DFT methods has been reported to be close to that computed through G2 method ($\pm 2-3$ kcal mol^{-1}).[36,43–45,50,51] Accidentally, an unusually large error (10 kcal mol^{-1}) is involved in $\Delta H^0_{(3)}$ at the B3LYP level and may be realized by the large combined deviation from experiment with the same theory predicted for the atomization energies of the individual reactants (overestimated by 4.5 kcal mol^{-1}) and products (underestimated by 4.4 kcal mol^{-1}) in reaction (3).[27(a)]

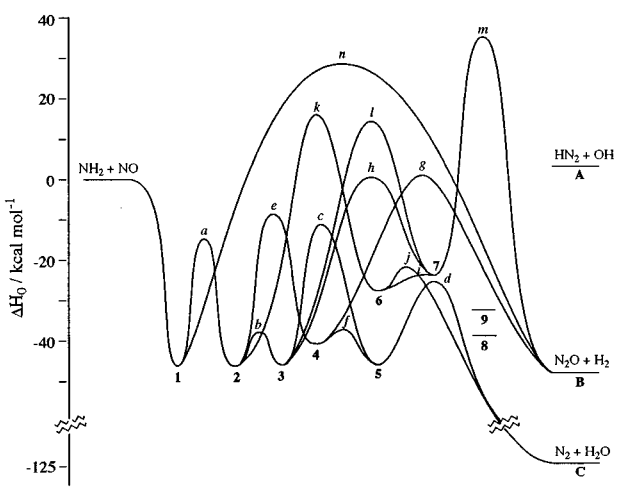

FIG. 3. The overall profile of potential energy surface for the NH_2+NO reaction predicted at the G2M(CC1) level of theory. The possible transition states involving intermediates **8** and **9** are not shown in the plot (refer to Table I for their detailed energetics). Note that the intermediates **2**–**7** can directly dissociate to form the radical products **A** (HN_2+OH) with no barrier other than their corresponding endothermicities.

The enthalpy $\Delta H^0_{(1)}$ of reaction (1) has been identified as playing an essential role in determining the branching ratio α via μVRRKM calculations.[25] This reaction is a standard open shell system which contains four radicals for the reactants and products. Thus, a problem arises from the serious spin contamination of the unrestricted wavefunctions for the open shell species (particularly for HN_2 radical in our case) which makes the energy evaluations less reliable.[52–56] Table III shows the details of the G2 calculations for the most important species of this system. $\Delta H^0_{(1)}$ at the G2M level is predicted to be 3.6 kcal mol^{-1}. It was obtained based on a relative PMP4 energy (7.9 kcal mol^{-1}) with further corrections for basis set incompleteness, electron correlation, and ZPE. Note that the HLC correction gives no contribution to the G2M energy because no net chemical bond is formed in reaction (1). Experimental data of $\Delta H^0_{(1)}$ is unavailable for this reaction owing to the very short lifetime of the HN_2

TABLE III. Summary of the detailed G2 calculations for the key species involved in the reaction between NH_2 and NO.[a,b]

	E_{total}[c]	Relative energy[d]/kcal/mol^{-1}						
	NH_2+NO	N_2+H_2O	HN_2+OH	H_2NNO, **1**	TS *a*	TS *c*	TS *g*	TS *h*
E(MP4)	−185.400 28	−119.91	+7.89	−43.92 (−44.64)	−11.69	−2.40	+1.88	+14.18 (+10.88)
$\Delta E(+)$	−0.011 03	−2.76	−1.19	−0.65 (−0.44)	+0.77	−3.48	+1.49	−10.06 (−9.20)
$\Delta E(2df)$	−0.092 25	+0.07	+0.64	−4.01 (−3.56)	−4.76	−4.64	−4.38	−2.76 (−1.88)
ΔE(CC)	+0.005 69	−0.33	−3.04	−0.21 (+0.37)[e]	+1.11	−0.66	+5.91	−0.08 (+1.77)[e]
ΔE(G2)	−0.012 80	−0.06	+0.45	−0.06 (+0.01)	+0.33	+0.14	+0.72	+0.34 (+0.27)
HLC	−0.048 06	−3.50	0.00	−3.50 (−2.92)[f]	−3.50	−3.50	−3.50	−3.50 (−2.92)[f]
ZPE	+0.023 41	+2.18	−1.16	+5.61 (+6.28)[g]	+2.95	+3.66	+0.49	+2.66 (1.48)[g]
E(G2)[h]	−185.535 32	−124.31	3.59	−46.74 (−44.90)	−14.79	−10.88	2.61	0.78 (0.40)

[a]Definition of the addivity scheme for the G2M(CC1) approach: E(MP4)=E[PMP4/6-311G(d,p)], $\Delta E(+)E$[PMP4/6-311+G(d,p)]-E(MP4), $\Delta E(2df)=E$[PMP4/6-311G($2df,p$)]-E(MP4), ΔE(CC)=E[CCSD(T)/6-311G(d,p)]-E(MP4), ΔE(G2)=E[PMP2/6-311+G($3df,2p$)]-E[PMP2/6-311G($2df,p$)]-E[PMP2/6-311+G(d,p)]+E[PMP2/6-311G(d,p)], HLC=$(-5.77n_\beta-0.19n_\alpha)/1000$, and the ZPE calculated at the B3LYP/6-311G (d,p) level of theory.
[b]The values in parentheses are the results obtained from the G2(PU) calculations with the geometries optimized at the QCISD/6-311G(d,p) level of theory.
[c]Total energy in units of hartree.
[d]Energy relative to the reactants NH_2+NO.
[e]ΔE(QCI)=E[QCISD(T)/6-311G(d,p)]-E[PMP4/6-311G(d,p)].
[f]HLC=$(-4.81n_\beta-0.19n_\alpha)/1000$.
[g]ZPE carried out at the QCISD/6-311G(d,p) level of theory.
[h]E(G2)=E(MP4)+$\Delta E(+)+\Delta E(2df)+\Delta E$(CC)+$E$(G2)+HLC+ZPE.

species as estimated theoretically[57,58] and experimentally.[59] Therefore, further energy calculations for $\Delta H^0_{(1)}$ were also carried out at various levels of theory for comparison. The results are listed in Table IV. In theory, the data obtained at the highest *ab initio*/MO level, CCSD(T)/AUG-cc-pVQZ, is 2.4 kcal mol^{-1}, which is 1.2 kcal mol^{-1} lower than that of the G2M method [recall that G2M attempts to approach a CCSD(T)/6-311+G($3df,2p$) calculation]. The correlation consistent quadruple-zeta basis set of Dunning with polarization and diffuse functions on all atoms (AUG-cc-pVQZ) (Ref. 32) seems to be a current *ab initio* limit for the basis functions of the system (number of basis functions are 172, 160, 206, and 126 for NH_2, NO, HN_2, and OH, respectively). This result is in excellent agreement with that of a BAC-MP4,[20] and very close to, though still higher by 1.7 kcal mol^{-1} than that of CASSCF/ICCI.[22] On the other hand, $\Delta H^0_{(1)}$ predicted from the highest B3LYP level of the present study (B3LYP/AUG-cc-pVQZ) is 0.9 kcal mol^{-1}, which is in surprisingly good accordance with that of CASSCF/ICCI, partly due to the small effect of the spin contamination involved in the spin-unrestricted DFT wave functions.[52–54] It is also interesting to discover that another cost-effective approach similar to the G2 method using complete basis set extrapolation (CBS-QCI/APNO) (Ref. 40) gives 1.4 kcal mol^{-1}, a value in good agreement with that of our B3LYP limit and that of Walch's multireference method.[22]

TABLE IV. Comparison of the reaction enthalpy for NH_2+NO $\rightarrow HN_2$+OH with various levels of theory.

cMethod	ΔH^0 (0 K)/kcal mol^{-1}	Note
BLYP/6-311G(d,p)	3.0	a
B3LYP/6-311G(d,p)	1.8	a
B3LYP/6-311+G(d,p)	0.2	a
B3LYP/cc-pVQZ	1.2	a
B3LYP/AUG-cc-pVQZ	0.9	a
PMP4/6-311G(d,p)	6.5	a
PMP4/6-311+G(d,p)	5.4	a
PMP4/AUG-cc-pVQZ	5.6	a
QCISD/6-311G(d,p)	3.1	a
QCISD(T)/6-311++G($2df,p$)	2.9	a
CCSD(T)/6-311G(d,p)	3.5	a
CCSD(T)/6-311+G(d,p)	2.4	a
CCSD(T)/AUG-cc-pVQZ	2.4	a
G2Q	4.4	b
G2(PU)	3.9	b
G2M(CC1)	3.6	a
CBS-QCI/APNO	1.4	b
BAC-MP4	2.4	c
CASSCF/ICCI	0.7	d

[a]Present studies with ZPE corrections at the B3LYP/6-311G(d,p) level of theory.
[b]Present studies with ZPE corrections at the QCISD/6-311G(d,p) level of theory.
[c]Reference 20.
[d]Reference 22.

B. Intermediate H_2NNO, 1

The intermediate **1** can be formed by the association of the NH_2 and NO radicals with a bond energy (at 0 K) of 44.2 kcal mol^{-1} at the B3LYP/cc-pVQZ+ZPE level (see Table I). Calculations performed at the PMP4/6-311G(d,p)+ZPE and CCSD(T)/6-311G(d,p) + ZPE levels give −38.3 and − 38.5 kcal mol^{-1}, respectively, for the relative energy of **1** with respect to reactants. However, the G2M approach effectively reduces the relative energy of **1** by 8.4 kcal mol^{-1} from the PMP4 energy and gives a value of −46.7 kcal mol^{-1}, mainly through the corrections of $\Delta E(2df)$ and HLC, as summarized in Table III. Our G2M energy of **1** is slightly higher by 1.4 kcal mol^{-1} than that of BAC-MP4,[20] but lower by 2.7 kcal mol^{-1} than

TABLE V. Comparison of optimized geometries (in Å and deg) and normal vibrational frequencies (in cm^{-1}) for H_2NNO **1** with various levels of theory.

	B3LYP/ 6-311G(d,p)[a]	B3LYP/ 6-311G+(d,p)[a]	HF/ 6-31G(d)[b]	HF/ 6-311G(d,p)[a]	MP2/ 6-311G(d,p)[a]	QCISD/ 6-311G(d,p)[a]	CAS(8,6)/ DZP[c]	CAS(12,11)/ cc-pVDZ[d]
H^1N^1	1.007	1.008	0.994	0.992	1.006	1.008	1.003	1.005
H^2N^1	1.018	1.018	1.000	0.999	1.016	1.015	1.029	1.022
N^1N^2	1.333	1.330	1.316	1.315	1.342	1.354	1.344	1.375
N^2O	1.213	1.214	1.184	1.175	1.221	1.208	1.201	1.219
$\angle H^1N^1N^2$	117.2	116.9	115.4	115.7	115.2	113.6	112.2	114.7
$\angle H^2N^1N^2$	119.5	120.1	117.3	117.8	117.4	115.5	113.9	117.6[e]
$\angle N^1N^2O$	114.2	114.5	114.5	114.8	113.4	113.5	113.5	113.4
$\angle ON^2N^1H^2$	0.0	0.0	13.4	11.9	12.3	17.1	20.7	21.0
$\angle H^1N^1N^2O$	180.0	180.0	164.8	166.7	166.2	160.7	155.4	157.8
ω_1	190	264	370	308	327	441	542	507
ω_2	632	633	690	692	633	619	647	597
ω_3	723	710	744	740	701	689	712	681
ω_4	1093	1097	1251	1239	1119	1091	1207	1056
ω_5	1223	1224	1392	1377	1266	1271	1368	1288
ω_6	1580	1578	1781	1761	1595	1621	1709	1616
ω_7	1609	1605	1882	1875	1613	1649	1792	1656
ω_8	3455	3459	3772	3752	3536	3536	3490	3534
ω_9	3697	3694	3955	3944	3756	3733	3871	3980

[a]Present work.
[b]Reference 21.
[c]Reference 22.
[d]Reference 23.
[e]$\angle H^1N^1H^2$.

that of CASSCF/ICCI (Ref. 1).[22] Note that the Ref. 1 column of the CASSCF/ICCI calculations shown in Table I is the result computed based on the experimental enthalpy of reaction (2) [$\Delta H^0_{(2)} = -47.2$ kcal mol^{-1}],[26] and the Ref. 2 column is the original result based on the relative energy of **1** calculated at the (6e in 6MOs) CASSCF/ICCI level (which gives -38.1 kcal mol^{-1} with regard to the reactants). The error in calculating NN bond strength using the CASSCF/ICCI technique was noticeably as large as 6 kcal mol^{-1}, which has also been pointed out by Walch,[22] mostly due to the incompleteness of the basis set as well as the insufficiency of the active space employed.

A previous *ab initio* study by Harrison *et al.*[21] implies that the inclusion of polarization functions at the Hartree–Fock (HF) level results in a nonplanar structure for **1**. However, the geometry of **1** predicted using the B3LYP method gives a *Cs* symmetry, regardless of the effects of the polarization or the diffuse functions included in the basis set. Table V shows the comparison of the structure and the corresponding vibrational frequencies for **1** with various levels of theory. It is apparent that the *ab initio*/MO methods with relatively large polarized basis functions through either a dynamic (e.g., MP2, QCISD, etc.) or a nondynamic (e.g., CASSCF) approach predict a nonplanar structure for **1**, but the B3LYP method gives a planar one. The planar equilibrium structure of **1** predicted at the B3LYP/6-311G(d,p) level has a much lower frequency (190 cm^{-1}) corresponding to an out-of-plane bending vibrational mode than that predicted by the *ab initio*/MO methods (which give 327, 441, 542, and 507 cm^{-1} at the MP2, QCISD, 8-in-6 CASSCF, and 12-in-11 CASSCF levels, respectively). Note that the former vibration has an A'' symmetry. Further inclusion of the diffuse functions for all non-hydrogen elements with the B3LYP method gives a very similar structure of **1** with the vibrational frequencies very close to the former prediction except for the first bending mode (264 cm^{-1}). Therefore, the planar equilibrium structure of **1** is a genuine prediction of the B3LYP method. Further study for the MEP of **1** dissociating into two reactant fragments indicates that the *Cs* symmetry of **1** has been broken into a C_1 symmetry along the NN bond-length reaction coordinate.[42]

In order to confirm the reliability of the energy prediction via the G2M method which was based on a planar B3LYP/6-311G(d,p) structure for intermediate **1**, further investigations have also been carried out using G2Q or G2(PU) approach based on a nonplanar QCISD/6-311G(d,p) structure for **1**. G2Q is a modified G2 method for the purpose of precisely predicting the energetics of transition states involving difficult open shell species based on the geometries and ZPE calculated at the QCISD/6-311G(d,p) level.[34,53] G2(PU) is used for the same purpose as G2Q but using the PMP4 method instead of only UMP4 (there is no difference using either PMP4 or UMP4 method for the close shell species) for the various levels of the energy corrections to better improve the uncertainties caused by the spin contamination of the open shell species [original G2(PU) was based on the geometry and ZPE calculated at the UMP2/6-311G(d,p) level].[35] The results of the relative energy of **1** are -44.8 and -44.9 kcal mol^{-1}, predicted at the G2Q and G2(PU) levels, respectively. Because **1** is a closed shell species, the excellent agreement in the energy prediction between G2Q and G2(PU) indicates that the effect of further corrections using PMP4 instead of UMP4 methods for the open shell reactants (NH_2 and NO radicals) was negligible. The energy of **1** pre-

dicted at the G2(PU) level is in a good agreement with, but somewhat higher by 1.8 kcal mol^{-1} than, that of G2M(CC1) due to the smaller negative corrections for both basis-set incompleteness and HLC (by definitions) as well as the larger positive corrections for both electron correlation [QCISD(T) vs CCSD(T)] and ZPE [QCISD/6-311G(d,p) vs B3LYP/6-311G(d,p)], as summarized in Table III. The G2(PU) result, which was calculated based on a nonplanar structure for **1**, is in excellent agreement with that of CASSCF/ICCI performed by Walch.[22]

C. Intermediates HNNOH, 2–5, and their corresponding transition states

The equilibrium structures of the intermediate HNNOH **2** as well as its three conformations, **3**, **4**, and **5** have the same *Cs* symmetry. The energetics of **2**, **3**, and **5** are quite similar at the G2M level, lying between -46.0 and -46.6 kcal mol^{-1} relative to the reactants, whereas **4** is endothermic by about 6 kcal mol^{-1} with respect to the others at the same level. Apparently, the relative energies predicted at the G2M level are in excellent agreement with those of BAC-MP4 within ± 1 kcal mol^{-1} for **2–5**, and agree very well with those of CASSCF/ICCI (Ref. 1) within ± 1.5 kcal mol^{-1} for **2**, **3**, and **5**, as shown in Table I.

Based on the results of the recent *ab initio* studies for the system,[19–23] the intermediate **1** would probably undergo a 1,3-hydrogen migration to form a *trans–cis* HNNOH isomer, **2**, through a four-member-ring transition state, TS *a*. The torsional barrier heights corresponding to both (**2,3**) and (**4,5**) isomer pairs have been predicted to be less than 10 kcal mol^{-1} through TS *b* and TS *f*, respectively.[21,22] Therefore, the following reaction rate determining steps after **2** is formed would be the isomerization processes between the (**2,3**) and (**4,5**) isomer pairs through the corresponding transition states, TS *e* (**2→4**) or TS *c* (**3→5**). Once the (**4,5**) isomer pair has been formed, the reaction could easily proceed to reach the final products N_2+H_2O (**C**) through TS *d* with a relatively low barrier. Another channel generating the radical products HN_2+OH (**A**) could also be accessed via direct dissociation of any of the intermediates **2–5**.[42]

The present study has confirmed this key kinetic mechanism by calculating the other possible processes at various levels of theory, i.e., the isomerization/dissociation of **1** to form intermediate OHNNH, **8**, and the products N_2O+H_2 (**B**) through TS *o* and TS *n*, respectively. The geometries and energetics are shown in Fig. 2 and Table I, respectively. The relative energies for TS *a*, TS *n*, and TS *o* are -14.8, 28.8, and 12.8 kcal mol^{-1}, respectively, according to the G2M predictions. Obviously, intermediate **1** would follow the reaction path via TS *a* to form **2** as expected.

As discussed previously, the key reaction path of this system could be presented as $NH_2+NO \rightarrow H_2NNO$ **1** $\rightarrow$TS*a*$\rightarrow$HNNOH (**2,3**)$\rightarrow$TS *c*/TS *e*$\rightarrow$HNNOH (**4,5**)$\rightarrow$TS *d*$\rightarrow N_2+H_2O$(**C**). Therefore, the corresponding transition states, in particular TS *a* and TS *c* (or TS *e*), would certainly play an important role for evaluating the reaction rate for the system via RRKM theory. The relative energy of TS *a* calculated at the G2M level (-14.8 kcal mol^{-1}) is in reasonable accordance with that of B3LYP/cc-pVQZ+ZPE(-12.6 kcal mol^{-1}) and agrees excellently with that of CASSCF/ICCI (Ref. 1, -14.4 kcal mol^{-1}). However, the result for TS *a* obtained via the BAC-MP4 method is 4.9 kcal mol^{-1} in energy lower than that of G2M, partly due to the inappropriate empirical bond additivity corrections employed for the transition states. Our results also show that TS *c* lies about 3 kcal mol^{-1} below TS *e* at both B3LYP and G2M levels, which indicates that the process involving **3→5** through TS *c* would be preferable for the kinetic model. The relative energy of TS *c* at the G2M level is -10.9 kcal mol^{-1}, which is lower by 2.9 and 2.5 kcal mol^{-1} than that predicted via BAC-MP4 and CASSCF/ICCI (Ref. 1) techniques, respectively.

The comparison of the optimized geometries and vibrational frequencies for both TS *a* and TS *c* with various levels of theory is shown in Table VI. Both TS *a* and TS *c* have been predicted to have a *Cs* symmetry. As for TS *a*, it is interesting that its geometry optimized at the B3LYP/6-311G(d,p) level is quite similar to that of optimized at the QCISD/6-311G(d,p) level,[61] and very close to that of predicted by Duan and Page at the 12-in-11 CASSCF/cc-pVDZ level of theory.[23] Both B3LYP and QCISD methods also give a very close prediction for the vibrational frequencies of TS *a*, however, the former is much preferred in terms of central processing unit (cpu) time. The vibrational frequencies of TS *a* predicted at the 8-in-6 and 12-in-11 CASSCF levels are about 8% and 3%, respectively, higher in average than those of the B3LYP method. With regard to the optimized structure of TS *c*, the N^2O bond length is predicted to be 1.54, 1.49, 1.61, and 1.55 Å with calculations at the B3LYP, QCISD, 10-in-10 CASSCF, and 12-in-11 CASSCF levels, respectively. Both B3LYP and 12-in-11 CASSCF techniques provide a very similar prediction for the geometry and vibrational frequencies of TS *c*. Although the B3LYP geometry of TS *c* is somehow looser than that of QCISD, their predicted vibrational frequencies are quite similar. The 10-in-10 CASSCF geometry of TS *c* is looser than that of B3LYP, thus, it gives lower values in average for the normal vibrational frequencies than the others, especially for the first two bending modes (corresponding to the N^2O motions). Once again, the performance of the B3LYP method in predicting the optimized geometries and the vibrational frequencies for the transition states is very impressive in comparison with those high-level quadratic configuration interaction and multireference methods.

It is widely understood that the energy barrier of TS *c* (or TS *e*) is much higher than that of TS *b* (or TS *f*) since the former involves a regular *cis–trans* isomerization for the hydrogen fragment moving inversely about the NN double bond on the same plan (C_s symmetry), whereas the latter involves a torsional motion for the hydroxyl fragment rotating along the NO single bond (C_1 symmetry). Instead of the torsional motions in the latter case, the hydroxyl fragment may also move into the other side of the NN double bond on the same plan (C_s symmetry). This process would give another two transition states, TS *u* (**2→5**) and TS ν (**3→4**).

TABLE VI. Comparison of optimized geometries (in Å and deg) and normal vibrational frequencies (in cm^{-1}) for the transition states *a* and *c* with various levels of theory.

	TS *a*				TS *c*			
	B3LYP/ 6-311G(d,p)[a]	QCISD/ 6-311G(d,p)[b]	CAS(8,6)/ DZP[c]	CAS(12,11)/ cc-pVDZ[d]	B3LYP/6-311G(d,p)[a]	QCISD/ 6-311G(d,p)[b]	CAS(10,10)/ DZP[c]	CAS(12,11)/ cc-pVDZ[d]
H^1N^1	1.019	1.017	1.007	1.005	0.994	0.992	0.991	0.985
N^1N^2	1.270	1.273	1.260	1.287	1.175	1.187	1.193	1.193
N^2O	1.281	1.284	1.258	1.292	1.540	1.494	1.606	1.554
H^2O	1.356	1.351	1.376	1.359	0.967	0.962	0.981	0.977
$\angle H^1N^1N^2$	117.8	117.8	118.5	117.8	173.9	175.1	174.5	174.7
$\angle N^1N^2O$	103.5	102.9	104.5	103.4	111.2	110.9	109.3	110.9
$\angle H^2ON^2$	78.4	77.5	78.6	78.1	100.6	100.7	100.3	99.5
ω_1	1893*i*	2052*i*	1990*i*	2049*i*	1250*i*	1389*i*	1359*i*	1370*i*
ω_2	584	534	629	619	422	418	344	414
ω_3	954	972	1006	974	476	496	389	435
ω_4	1175	1182	1207	1197	503	546	576	518
ω_5	1219	1210	1348	1217	674	716	595	654
ω_6	1374	1375	1562	1392	1220	1290	1194	1244
ω_7	1464	1497	1642	1499	1878	1836	1793	1804
ω_8	2072	2180	2160	2134	3784	3860	3688	3674
ω_9	3493	3573	3791	3778	3877	3938	4030	4067

[a]Present work.
[b]Reference 61.
[c]Reference 22.
[d]Reference 23.

However, the possibility for this type of transition would be very slim because a very high energy barrier was predicted (see Table I).

Most previous kinetic studies[11,25] for this reaction assumed that TS *c* is the bottleneck of leading to the final product group **C** due to the relatively low energy barrier of TS *d*. No attempts have been made thus far to interpret the kinetic data for the possible product group **B** owing to the large barrier height of TS *n* previously predicted by BAC-MP4.[20] Recently, a new transition state, TS *g* (**4→B**), was predicted by Duan and Page using the 12-in-11 CASSCF wave function and the cc-pVDZ basis set.[23] However, their further single-point energy calculation for TS *g* was only carried out at a HF reference CI level due to the impracticability of implementing a MR-CI method for the system with such large reference space (about 61 000 singlet configurations in the MCSCF expansion). The PES of the system characterized at the SCF-CI/cc-pVTZ//12-in-11 CASSCF/cc-pVDZ level is comparable with that calculated at the MP4SDQ/6-31G(d)//HF/6-31G(d) level,[21] as shown in Table I. Therefore, it is demanded in this study to provide a more accurate prediction for the energetics of TS *g* so that one may be able to quantitatively account for the high-temperature shock tube data for reaction (2) using the μVRRKM theory.[62]

TS *g* is a five-member-ring saddle point with a planar structure (C_s symmetry), as shown in Fig. 2. For comparison, the geometry and normal vibrational frequencies of TS *g* calculated at the B3LYP/6-311G(d,p), MP2/6-311G(d,p), QCISD/6-311G(d,p), and 12-in-11 CASSCF/cc-pVDZ levels of theory are summarized in Table VII. All B3LYP, QCISD, and CASSCF methods give a very similar prediction for the optimized structure and the vibrational frequencies of TS *g*, whereas the MP2 method predicted a reasonably accordant geometry but with the vibrational frequencies higher by about 5% in average than the others. Based on the geometry optimized at the B3LYP/6-311G(d,p) level, the relative energy of TS *g* is predicted to be 3.6, 2.4, 8.3, and 2.6 kcal mol^{-1} at the B3LYP/cc-pVQZ+ZPE, PMP4/6-311G(d,p)+ZPE, CCSD(T)/6-311G(d,p) + ZPE, and G2M levels, respectively. Note that the CCSD(T) result is higher by 5.9 kcal mol^{-1} than that of the PMP4 method. It can also be seen from Table III that the positive corrections of ΔE(CC) and $\Delta E(+)$ tend to compensate with those of $\Delta E(2df)$ and HLC and make almost no net energy corrections for the G2M result with respect to that of the original (PMP4 with ZPE). This compensation effect for the G2M energy corrections can be rationalized due to the tight structures of the closed ring transition states (TS *a* is another example but with less effect).

On the other hand, the G2M energy of TS *g* is significantly lower by 26.2 kcal mol^{-1} than that of TS *n* predicted at the same level. Therefore, the possible reaction path of generating N_2O and H_2 products for the system could be presented as NH_2+NO→H_2NNO **1**→TS *a*→HNNOH (**2,3**)→TS *c*/TS *e*→HNNOH (**4,5**)→TS *g*→N_2O+H_2 (**B**). Once (**4,5**) has been formed, the competition among the three channels (**A**, **B**, and **C**) would be governed by the following corresponding steps:

$$\text{HNNOH}(\mathbf{4,5}) \rightarrow \text{MEP} \rightarrow \text{HN}_2 + \text{OH}(\mathbf{A}), \tag{4}$$

$$\text{HNNOH}(\mathbf{4,5}) \rightarrow \text{TS } g \rightarrow \text{N}_2\text{O} + \text{H}_2(\mathbf{B}), \tag{5}$$

$$\text{HNNOH}(\mathbf{4,5}) \rightarrow \text{TS } d \rightarrow \text{N}_2 + \text{H}_2\text{O}(\mathbf{C}), \tag{6}$$

TABLE VII. Comparison of optimized geometries (in Å and deg) and normal vibrational frequencies (in cm^{-1}) for the transition states *g* and *h* with various levels of theory.

	TS *g*				TS *h*				
	B3LYP/ 6-311G(*d*,*p*)[a]	MP2/ 6-311G(*d*,*p*)[a]	QCISD/ 6-311G(*d*,*p*)[a]	CAS(12,11)/ cc-pVDZ[b]	B3LYP/ 6-311G(*d*,*p*)[a]	B3LYP/ 6-311+G(*d*,*p*)[a]	MP2/ 6-311G(*d*,*p*)[a]	MP2/ 6-311+G(*d*,*p*)[a]	QCISD/ 6-311G(*d*,*p*)[a]
H^1H^2	0.957	0.975	0.936	1.009					
H^1N^1	1.458	1.408	1.483	1.453	1.029	1.025	1.027	1.024	1.035
N^1N^2	1.177	1.194	1.181	1.178	1.132	1.124	1.172	1.160	1.146
N^1O					2.142	2.193	2.153	2.182	2.212
N^2O	1.242	1.243	1.248	1.254	2.226	2.237	2.159	2.155	2.328
H^2O	1.436	1.395	1.404	1.382	0.974	0.970	0.976	0.975	0.970
$\angle H^1N^1N^2$	92.8	91.1	92.2	94.0	135.4	141.3	129.3	137.2	128.3
$\angle N^1N^2O$	128.1	127.3	127.6	126.5	70.9	73.1	74.0	75.8	69.8
$\angle H^2ON^1$					168.2	170.5	176.5	177.2	165.5
$\angle H^2ON^2$	89.2	90.5	88.8	90.9	161.8	160.2	152.0	151.7	165.4
$\angle H^1H^2O$	118.5	115.6	122.1						
ω_1	1502*i*	1461*i*	1767*i*	1956*i*	533*i*	466*i*	544*i*	459*i*	451*i*
ω_2	769	801	760	806	394	409	396	371	235
ω_3	776	904	822	865	426	433	434	461	247
ω_4	1118	1178	1100	1089	568	573	639	644	361
ω_5	1220	1284	1241	1245	728	576	839	703	721
ω_6	1297	1410	1276	1303	898	852	967	926	752
ω_7	1471	1468	1491	1510	2103	2139	1887	1895	2008
ω_8	1898	1996	1882	1929	3315	3400	3392	3473	3218
ω_9	2066	2086	2157	1957	3680	3749	3696	3717	3746

[a]Present work.
[b]Reference 23.

where the minimum energies (with respect to the reactants) required for the reactions (4), (5), and (6) are 3.6, 2.6, and -24.9 kcal mol^{-1}, respectively, at the G2M level. We believe that the reactions (6) and (4) would still respectively dominate the system under low and high temperature conditions[25] due to the advantage of energetics for the former and the loose transition state property for the latter. However, the reaction path of forming product group **B** through TS *g* might be relatively competitive under high-temperature shock tube conditions, which requires further kinetic investigation.[62]

D. Intermediates HOHNN, 6–7, and their corresponding transition states

The mechanism of the title reaction involving intermediate **6** or its torsional counterpart, **7** has not been well studied previously because a very high energy barrier was predicted to be responsible for a rate-determining step in the mechanism.[20] On the other hand, **6** and **7** were also predicted to be less stable by about 20 kcal mol^{-1} than their other isomers (**2–5**).[18,20] In this study, we have carefully examined the possible transition states with relation to **6** or **7** which may be kinetically involved in the reaction mechanism for the system. The structures and the energetics of **6** and **7** will be discussed first before we elaborate on the corresponding transition states and the possible reaction mechanism.

Intermediate **6** as well as **7** has a planar geometry with C_s symmetry and a $^1A'$ ground electronic state, as shown in Fig. 1. The bond length of N^1N^2 and N^1O for **6** (or **7** in parentheses) was predicted to be 1.157 (1.152) and 1.545 (1.575) Å, respectively, at the B3LYP/6-311G(*d*,*p*) level of theory. The Mulliken population analysis gives the charges $+0.29$ ($+0.28$) *e* and -0.15 (-0.12) *e* for the N^1 and N^2 atoms of **6** (or **7**), respectively. This is the reason why the N^1O distance is longer than a regular NO single bond, and the N^1N^2 bond length is between the regular values for the double and triple NN bonds. The ionic property of the intermediates **6** and **7** is similar to that of the HNN(OH)O isomers involved in the NH_2+NO_2 reaction recently studied by the Mebel *et al.*[35(a)] The relative energies of **6** (or **7** in parentheses) are -25.7 (-21.1) and -28.0 (-23.3) kcal mol^{-1} calculated at the B3LYP/cc-pVQZ+ZPE and G2M levels, respectively. The torsional energy barrier between 6 and 7 was predicted to be negligible with respect to **7** with ZPE corrections included, where the corresponding transition state, TS *i* (**6→7**), has a nonplanar structure as expected.

We now focus on what would happen once the (**6,7**) isomer pair is formed. Firstly, direct dissociation of either **6** or **7** would lead to product group **A** with no barrier other than the endothermicity (31.6 and 26.9 kcal mol^{-1} for **6** and **7**, respectively, at the G2M level). Secondly, the two H atoms of **7** could come closer to form **B** products, however, this possibility is very unlikely since a high energy barrier is responsible for the corresponding transition state, TS *m* (**7→B**). Thirdly, a transition between **6** and **8** may occur via a 1,3-hydrogen migration with the corresponding transition state (TS *t*) lying above the reactants by 7.1 kcal mol^{-1}. Finally, the O atom of **6** may catch the H atom on the other side of the NN bond to form **C** products. This process is characterized by the corresponding transition state, TS *j* (**6→C**). The structure of TS *j* is nonplanar with H, N, and O atoms forming a loose three-membered ring, as

shown in Fig. 2. The IRC calculations confirm TS *j* to connect **6** with channel **C**. The relative energy of TS *j* was estimated to be less than -4.3 kcal mol^{-1},[20] however, the more accurate G2M method has predicted a much lower value, -20.4 kcal mol^{-1}. Therefore, it would only require 7.6 kcal mol^{-1} to surmount the energy barrier (with ZPE) for **6** leading to product group **C** based on the G2M prediction. According to the energetics of different possible channels discussed here, it strongly suggests that the reaction would most likely proceed to generate the products H_2O and N_2 once the (**6,7**) isomer pair is formed. As a result, it would be very curious to see which step effectively leads to the intermediate pair (**6,7**), and how important kinetically it could be.

In principle, there are two types of transitions which could connect HNNOH (**2–5**) and HOHNN (**6–7**), the first is a 1,2-H shift, and the second a 1,2-OH shift. Two transition states, TS *k* (**2→6**) and TS *l* (**3→7**), have been found for the former case. These 1,2-hydrogen migration processes in fact give high energy barriers as one may expect (TS *k* and TS *l* lie above the reactants by 16.6 and 14.8 kcal mol^{-1}, respectively, both predicted at the G2M level). For the latter case, a challenging transition state (TS *h*) with a nearly equilateral-triangular geometry has been discovered. TS *h* has a loose planar structure with the distance of N^1O and N^2O predicted to be 2.14 and 2.23 Å, respectively, as shown in Fig. 2. The H^2 atom of TS *h* is located immediately above the ON^1N^2 triangular ring. One may guess that TS *h* is responsible for either the transition **2→7** or **3→6** if the H^2 atom is assumed to be on the same side of the two corresponding isomers during the OH migration process. However, the IRC calculations have confirmed that TS *h* is exactly a saddle point connecting two minimums between **3** and **7** with the 1,2-OH migration corresponding to an internal rotation. This can be further rationalized by checking its imaginary vibrational frequency (ω_1) listed in Table II. The value of ω_1 for TS *h* is 533*i*. The low absolute value is expected since its reaction coordinate involves a rotational motion. The other similar examples are TS $b(587i)$, TS $f(484i)$, and TS $i(230i)$ with correspondingly low imaginary frequencies responsible for the torsional motions of the reaction coordinates.

The relative energy of TS *h* is predicted to be 15.5, 11.5, 16.8, 16.8, and 0.8 kcal mol^{-1} at the B3LYP/6-311G(d,p)+ZPE, B3LYP/cc-pVQZ+ZPE, PMP4/6-311G(d,p)+ZPE, CCSD(T)/6-311G(d,p) + ZPE, and G2M(CC1) levels of theory, respectively. It is surprising again that the G2M approach significantly reduces the PMP4+ZPE relative energy by as much as 16.0 kcal mol^{-1}! It can be recognized from Table III that the most significant correction in the G2M calculations for TS *h* comes from $\Delta E(+)$, which gives a $-$ 10 kcal mol^{-1} correction obtained from the relative energy difference between the PMP4/6-311+G(d,p) and PMP4/6-311G(d,p) levels. Diffuse functions are usually augmented to the standard basis set for a proper description of the anionic species.[29,39,50] However, our result suggests that the incorporation of diffuse functions in the basis set seems also to be necessary for a better description of a transition state with a loose structure like TS *h*. In order to further confirm the B3LYP geometry, we optimized TS *h* at the MP2 and QCISD levels of theory with the 6-311G(d,p) basis set, and additional diffuse functions for all nonhydrogen elements were also augmented for the B3LYP and the MP2 methods. The results of optimized geometries and vibrational frequencies of TS *h* calculated at these levels of theory are summarized in Table VII. One can see that both B3LYP and MP2 give similar results, and the distances of N^1O and N^2O are only lengthened by 0.05 (0.03) and 0.01 (0.00) Å, respectively, with additional diffuse functions augmented at the B3LYP (or MP2 in parentheses) level. This is not expected to affect the energy much. The geometry of TS *h* optimized at the QCISD/6-311G(d,p) level would lead to a looser structure, with the N^1O and N^2O bonds being, respectively, 0.07 and 0.10 Å longer than those computed at the B3LYP/6-311G(d,p) level. This is also expected to have only a minor effect on the energy. However, the force constants of TS *h* calculated at the QCISD level give somewhat lower vibrational frequencies than those obtained at the B3LYP and MP2 levels (particularly for the first three bending modes shown in Table VII). These lower vibrational frequencies would of course give a smaller ZPE correction for TS *h*. Furthermore, they would certainly influence the kinetics through affecting the sum of states at the transition state. A G2(PU) calculation was carried out based on this QCISD geometry to confirm the energetics for TS *h*. The result of G2(PU), summarized in Table III, is in excellent agreement with that of G2M, which indicates that the geometry of TS *h* optimized at a different level of theory does not significantly alter the energy according to the G2 results.

The large $\Delta E(+)$ contribution (-9.2 kcal mol^{-1}) in the G2(PU) calculations of TS *h* is also noteworthy. However, this energy correction is based on a PMP4 calculation. Clearly the PMP4 calculation with the diffuse functions augmented would give a much lower relative energy for TS *h* than that without diffuse functions. Therefore the uncertainty for the additivity scheme of the diffuse functions utilized in these G2 methods for TS *h* needs to be verified. In order to confirm this point, we directly calculated a single point energy for TS *h* as well as the reactants at the QCISD(T)/6-311+G(d,p) level based on the QCISD geometry. The $\Delta E(+)$ obtained from the relative energy difference between the QCISD(T)/6-311+G(d,p) and the QCISD(T)/6-311G(d,p) levels was only -6.0 kcal mol^{-1}, a value higher by 3.2 kcal mol^{-1} in energy than that predicted from traditional G2(PU) scheme.[63] This result implies that the relative energy of TS *h* predicted by G2M or G2(PU) method may involve an uncertainty more than -3 kcal mol^{-1} due to their overestimation for the $\Delta E(+)$ based on the additivity scheme calculated at the PMP4 level. This deviation was also recognized in recent G2 studies for the small anionic systems.[39,64] A simpler but more expensive additivity scheme, the G2(DD) approach, was suggested by Gronert[39] for properly describing anionic species. We thus modified the G2(DD) method by further incorporating the HLC and ZPE corrections to improve the original G2 calculations for the loose TS *h* species,

$$
\begin{aligned}
E[\mathrm{G2(DD)}] = {} & \mathrm{CCSD(T)/6\text{-}311{+}{+}G}(d,p) \\
& + \mathrm{PMP4/6\text{-}311{+}{+}G}(2df,p) \\
& - \mathrm{PMP4/6{-}311{+}{+}G}(d,p) \\
& + \mathrm{PMP2/6\text{-}311{+}{+}G}(3df,2p) \\
& - \mathrm{PMP2/6{-}311{+}{+}G}(2df,p) \\
& + \mathrm{HLC} + \mathrm{ZPE}. \qquad (7)
\end{aligned}
$$

The effect of the extra diffuse functions added for the hydrogen atoms of TS *h* is predicted to be very small (-0.1 kcal mol^{-1}) since the loose triangle structure is composed of the other three nonhydrogen atoms. In Eq. (7), HLC (in mhartree) $= -xn_\alpha - 0.19n_\beta$, where n_α and n_β are the number of α and β valence electrons, respectively, with $n_\alpha \geqslant n_\beta$. In principle, x is an empirical coefficient based on the average absolute deviation of calculated atomization energies from experiment for the G2 sample set of molecules.[33] In this study, x is adopted to be 5.77 and 4.81 for the G2M (Ref. 37) and G2(PU) (Ref. 35) methods, respectively, and this would contribute -3.5 and -2.9 kcal mol^{-1} for the HLC in the relative energy of TS *h* for the former and the latter, respectively. According to Eq. (7), we calculated the relative energy for TS *h* based on the optimized geometries and ZPEs at the QCISD level and assumed $\Delta E(\mathrm{HLC}) = -3.5$ kcal mol^{-1}. This modified scheme gives 2.3 kcal mol^{-1}, which would be a better prediction to approximate the relative energy for TS *h* at the CCSD(T)/6-311++G$(3df,2p)$‖QCISD/6-311G(d,p) level with the HLC and ZPE corrections included.

The kinetic effect of TS *h* in the mechanism of the NH_2+NO reaction has not yet been discussed in the literature due to the large energy barrier (65 kcal mol^{-1} with respect to the reactants) predicted by the BAC-MP4 method.[20] Because the new TS *h* found in this study involves a low energy barrier with a loose structure, it may have some kinetic effect by contributing to channel **C** in combination with the processes through TS *c*/TS *e* and compete with the direct dissociation of either **2** or **3** leading to channel **A**,

$$\mathrm{HNNOH}(\mathbf{2,3}) \rightarrow \mathrm{MEP} \rightarrow \mathrm{HN_2} + \mathrm{OH}(\mathbf{A}), \qquad (8)$$

$$
\begin{aligned}
\mathrm{HNNOH}(\mathbf{2,3}) & \rightarrow \mathrm{TS}c/e \rightarrow \mathrm{HNNOH}(\mathbf{4,5}) \rightarrow \mathrm{TS}d \\
& \rightarrow \mathrm{N_2} + \mathrm{H_2O}(\mathbf{C}), \qquad (9)
\end{aligned}
$$

$$
\begin{aligned}
\mathrm{HNNOH}(\mathbf{2,3}) & \rightarrow \mathrm{TS}h \rightarrow \mathrm{HOHNN}(\mathbf{6,7}) \rightarrow \mathrm{TS}j \\
& \rightarrow \mathrm{N_2} + \mathrm{H_2O}(\mathbf{C}), \qquad (10)
\end{aligned}
$$

where reaction (8) is a simple bond dissociation step similar to reaction (4),[42] reaction (9) should be further considered in association with the reactions (4) and (5), and reaction (10) is clearly controlled by TS *h*. The TS *h* lies (15–18) kcal mol^{-1} higher in energy than TS *c* but has similar energetics with regard to channel **A**. Therefore, it may give some contribution to channel **C** via reaction (10) in competition with reaction (8) particularly under high temperature conditions. A multichannel μVRRKM calculation is required to demonstrate how important TS *h* would be in effecting the branching ratio α of the NH_2+NO reaction under $DeNO_x$ conditions.[62]

E. Intermediates OHNNH, 8–9, and their corresponding transition states

Different from intermediates **2**–**7**, the OHNNH isomers, **8** and **9**, cannot lead to channel **A** via direct bond dissociation steps. Therefore, both **8** and **9** are considered to be less important kinetically than the other isomers. At the G2M level, the relative energy of **8** and **9** are predicted to be -37.8 and -32.8 kcal mol^{-1}, respectively. The *cis–trans* isomerization between **8** and **9** involves a nonplanar transition state (TS *p*) with a relatively high energy barrier (-0.3 kcal mol^{-1} with regard to the reactants) similar to TS *c* or TS *e*. We have mentioned previously that intermediate **8** can be formed, respectively, from **1** or **6** through TS *t* or TS *o*, but both transition states involve a high energy barrier. Intermediate **9** can be generated from **3** via a 1,2-H shift (TS *r*) but still involves a high barrier. The high energies of the transition states for forming **8** or **9** implies that these intermediates are unlikely to be kinetically significant.

IV. CONCLUDING REMARKS

The PES for the reaction of the NH_2 with NO has been characterized using the B3LYP methods with a 6−311 G(d,p) basis set to locate the stationary points followed by the energy calculations at several levels of theory. In general, the relative energies of the species involved in the system calculated at the B3LYP level are much better than those at the PMP4 or the CCSD(T) level using the same basis set [6-311 G(d,p)] in comparison with the G2M results, as summarized in Table I. For instance, the mean absolute deviations between B3LYP and G2M energies are 5.1 and 3.8 kcal mol^{-1} for intermediates **1**–**9** and transition states *a*–*w*, respectively, whereas those between CCSD(T) and G2M energies are 10.1 and 9.7 kcal mol^{-1} for intermediates **1**–**9** and transition states *a*–*w*, respectively. Further calculations using a large basis set (cc-pVQZ) for the B3LYP method do not give a significant improvement in energy. The stability of the B3LYP energies was not very good due to a maximum deviation of 10 kcal mol^{-1} predicted for the enthalpy of reaction (3), however, the optimized geometries and the vibrational frequencies for the most important species calculated at such level are as good as those at the QCISD and 12-in-11 CASSCF levels. Interestingly, Walch's original CASSCF/ICCI (Ref. 2) results are in fact in excellent match with our energy predicted at the CCSD(T) level of theory, however, further energy adjustment by shifting -5.9 kcal mol^{-1} for all species with respect to the reactants based on the experimental enthalpy of reaction (2) makes Walch's results (Ref. 1) in agreement with our G2M predictions with uncertainties within ± 3 kcal mol^{-1}. On the other hand, the relative energies of the intermediates **1**–**9** predicted by the BAC-MP4 method are about 10 kcal mol^{-1} on average lower than our PMP4 results due to the large bond energy corrections made by the

former method. The BAC-MP4 results are basically in agreement with our G2M predictions for the intermediates and the product channels (**A**–**C**), but the relative energies predicted by BAC-MP4 for the transition states of the system appear to be inaccurate due to the insufficient geometry optimization at the HF level of theory with the relatively small basis set and the possibly inadequate bond additivity corrections for the transition states.

According to the present study, three product channels, **A**–**C**, should be involved in the reaction mechanism. For channel **A**, any one of the HNNOH (**2**–**5**) or HOHNN (**6**,**7**) isomers can directly dissociate into HN_2 and OH radicals with no barrier other than the corresponding endothermicities. For the kinetic purpose, the enthalpy of reaction (1) have been further investigated in this work. The results according to the predictions at our highest level are 0.9 and 2.4 kcal mol^{-1}, respectively, based on the B3LYP and CCSD(T) methods with a relatively large basis set (AUG-cc-pVQZ). The former and the latter are, respectively, in excellent accordance with that predicted at the CASSCF/ICCI and BAC-MP4 levels. The product channel **B** producing the N_2O and H_2 products may be reasonably reached at high temperatures via the rate-determining step involving a five-member-ring transition state (TS g,**4**→**B**) with an energy barrier of 2.6 kcal mol^{-1} relative to the reactants based on the G2M prediction. The previous shock tube result for this channel could not be properly accounted for since a three-member-ring transition state (TS n,**1**→**B**) with a much higher energy barrier had previously been assumed. The NH_2+NO reaction can reach the N_2 and H_2O products (channel **C**) with no intrinsic barrier. The rate-determining steps leading to channel **C** for the reaction were predicted to be the isomerization processes involving TS a(**1**→**2**) and TS c(**3**→**5**). The relative energies of TS a and TS c are -14.8 and -10.9 kcal mol^{-1}, respectively, predicted at the G2M level. Another channel of producing N_2+H_2O was found to involve a loose 1,2-OH migration with the corresponding transition state (TS h,**3**→**7**) lying above the reactants by 0.8 kcal mol^{-1} as predicted by the G2M method. TS h has a planar structure with the three nonhydrogen atoms forming a loose nearly equilateral triangle. The geometry optimized at the QCISD/6-311G(d,p) level gives a further loose structure for TS h together with three smaller bending vibrational frequencies, as shown in Table VII. The traditional G2M scheme underestimated the relative energy of TS h by 3.7 kcal mol^{-1} due to the inappropriate energy correction for the basis set incompleteness with additional diffuse functions for all nonhydrogen elements calculated using the PMP4 method. Therefore, an improved additivity scheme based on the G2(DD) approach for better describing TS h has been provided. We have utilized the G2(DD) method with HLC and ZPE corrections included to approach the energy calculation of TS h at the CCSD(T)/6-311++G($3df$,$2p$)//QCISD/6-311G(d,p) level of theory, where a relative energy of 2.3 kcal mol^{-1} was obtained at such level. The low energy barrier of TS h with respect to NH_2+NO, as well as its loose transition state characters, strongly suggests that there may exist another possibility for forming H_2O via the isomerization process involving TS h in competition with channel **A**, especially under high temperature combustion conditions.

ACKNOWLEDGMENTS

The authors gratefully acknowledge the support of this work by the Australian Research Council Large Grants Scheme (Grant No. A29532744). We are indebted to Dr. Ching-Han Hu and Professor Henry F. Schaefer III for many helpful suggestions and discussions. We wish to thank the referees for their very thorough reading of the manuscript and for the very helpful suggestions. E. W.-G. Diau wishes to thank Professors M. C. Lin, K. Morokuma and Dr. A. M. Mebel for many valuable suggestions and guidance of writing this paper. The helpful comments made by Dr. R. M. W. Wong are also much appreciated.

[1] R. K. Lyon, U.S. Patent No. 3 900 554, Int. J. Chem. Kinet. **8**, 315 (1976).
[2] J. A. Miller, M. C. Branch, and R. J. Kee, Combust. Flame **43**, 81 (1981).
[3] J. A. Miller and C. T. Bowman, Prog. Energy Combust. Sci. **15**, 287 (1989).
[4] P. Glarborg, K. Dam-Johansen, J. A. Miller, R. J. Kee, and M. E. Coltrin, Int. J. Chem. Kinet. **26**, 421 (1994).
[5] J. A. Miller and P. Glarborg, *Gas Phase Chemical Reaction Systems Experiments and Models 100 Years after Max Bodenstein*, Springer Series in Chemical Physics, 1996 (in press).
[6] J. A. Silver and C. E. Kolb, J. Phys. Chem. **86**, 3240 (1982).
[7] B. Atakan, A. Jacobs, M. Wahl, R. Weller, and J. Wolfrum, Chem. Phys. Lett. **155**, 609 (1989).
[8] V. P. Bulatov, A. A. Ioffe, V. A Lozovsky, and O. M. Sarkisov, Chem. Phys. Lett. **161**, 141 (1989).
[9] J. W. Stephens, C. L. Morter, S. K. Farhat, G. P. Glass, and R. F. Curl, J. Phys. Chem. **97**, 8944 (1993).
[10] M. Wolf, D. L. Yang, and J. L. Durant, J. Photochem. Photobiol. A: Chem. **80**, 85 (1994).
[11] E. W. Diau, T. Yu, M. A. G. Wagner, and M. C. Lin, J. Phys. Chem. **98**, 4034 (1994).
[12] J. Park and M. C. Lin, J. Phys. Chem. **100**, 3317 (1996).
[13] T. R. Roose, R. K. Hanson, and C. H. Kruger, in *Proceedings of the 18th International Symposium on Combustion, 1980* (The Combustion Institute, Pittsburgh, 1981), p. 853.
[14] M. A. Kimball-Linne and R. K. Hanson, Combust. Flame **64**, 337 (1986).
[15] J. Vandooren, J. Bian, and P. J. van Tiggelen, Combust. Flame **98**, 402 (1994).
[16] M. J. Brown and D. B. Smith, in *Proceedings of the 25th International Symposium on Combustion, 1994* (The Combustion Institute, Pittsburgh, 1995), p. 1011.
[17] M. J. Halbgewachs, E. W. G. Diau, A. M. Mebel, M. C. Lin, and C. F. Melius, in *Proceedings of the 26th International Symposium on Combustion, 1996* (The Combustion Institute, Pittsburgh, 1997) (in press).
[18] C. J. Casewit and W. A. Goddard, III, J. Am. Chem. Soc. **104**, 3280 (1982).
[19] H. Abou-Rachid, C. Pouchan, and M. Chaillet, Chem. Phys. **90**, 243 (1984).
[20] C. F. Melius and J. F. Binkley, in *Proceedings of the 20th International Symposium on Combustion, 1984* (The Combustion Institute, Pittsburgh, 1985), p. 575.
[21] J. A. Harrison, R. G. A. R. Maclagan, and A. R. Whyte, J. Phys. Chem. **91**, 6683 (1987).
[22] S. P. Walch, J. Chem. Phys. **99**, 5295 (1993).
[23] X. Duan and M. Page, J. Mol. Struct. (Theochem) **333**, 233 (1995).
[24] (a) L. F. Phillips, Chem. Phys. Lett. **135**, 269 (1987); (b) R. G. Gilbert, A. R. Whyte, and L. F. Phillip, Int. J. Chem. Kinet. **18**, 721 (1986).
[25] E. W.-G. Diau and Sean C. Smith, J. Phys. Chem. **100**, 12 349 (1996).
[26] M. W. Chase, Jr., C. A. Davies, J. R. Downey, Jr., D. J. Frurip, R. A. McDonald, and A. N. Syverud, *JANAF Thermochemical Tables*, J. Phys. Chem. Ref. Data **14** (1985).

[27] (a) A. D. Becke, J. Chem. Phys. **98**, 5648 (1993); (b) **97**, 9173 (1992); (c) **96**, 2155 (1992).
[28] C. Lee, W. Yang, and R. G. Parr, Phys. Rev. B **37**, 785 (1988).
[29] W. Hehre, L. Radom, P. v. R. Schleyer, and J. A. Pople, *Ab Initio Molecular Orbital Theory* (Wiley, New York, 1986).
[30] J. A. Pople, M. Head-Gordon, and K. Raghavachari, J. Chem. Phys. **87**, 5968 (1987).
[31] C. Gonzalez and H. B. Schlegel, J. Phys. Chem. **90**, 2154 (1989).
[32] (a) D. E. Woon and T. H. Dunning, Jr., J. Chem. Phys. **98**, 1358 (1993); (b) R. A. Kendall, T. H. Dunning, Jr., and R. J. Harrison, *ibid*. **96**, 6796 (1992); (c) T. H. Dunning, Jr., *ibid*. **90**, 1007 (1989).
[33] (a) L. A. Curtiss, K. Raghavachari, and J. A. Pople, J. Chem. Phys. **103**, 4192 (1995); (b) Chem. Phys. Lett. **214**, 183 (1993); (c) J. Chem. Phys. **98**, 1293 (1993); (d) L. A. Curtiss, K. Raghavachari, G. W. Trucks, and J. A. Pople, *ibid*. **94**, 7221 (1991); (e) L. A. Curtiss, C. Jones, G. W. Trucks, K. Raghavachari, and J. A. Pople, *ibid*. **93**, 2537 (1990).
[34] J. L. Durant, Jr. and C. M. Rohlfing, J. Chem. Phys. **98**, 8031 (1993).
[35] (a) A. M. Mebel, C.-C. Hsu, M. C. Lin, and K. Morokuma, J. Chem. Phys. **103**, 5640 (1995); (b) A. M. Mebel, K. Morokuma, M. C. Lin, and C. F. Melius, J. Phys. Chem. **99**, 1900 (1995); (c) A. M. Mebel, K. Morokuma, and M. C. Lin, J. Chem. Phys. **101**, 3916 (1994).
[36] C. W. Bauschlicher, Jr. and H. Partridge, J. Chem. Phys. **103**, 1788 (1995).
[37] A. M. Mebel, K. Morokuma, and M. C. Lin, J. Chem. Phys. **103**, 7414 (1995).
[38] (a) L. A. Curtiss, P. C. Redfern, B. J. Smith, and L. Radom, J. Chem. Phys. **104**, 5148 (1996); (b) B. J. Smith and L. Radom, J. Phys. Chem. **99**, 6468 (1995); (c) B. J. Smith and L. Radom, Chem. Phys. Lett. **245**, 123 (1995).
[39] (a) S. Gronert, Chem. Phys. Lett. **252**, 415 (1996); (b) J. Am. Chem. Soc. **115**, 10 258 (1993).
[40] (a) J. A. Montgomery, Jr., J. W. Ochterski, and G. A. Petersson, J. Chem. Phys. **101**, 5900 (1994); (b) G. A. Petersson, T. G. Tensfeldt, and J. A. Montgomery, Jr., *ibid*. **94**, 6091 (1991); (c) G. A. Petersson and M. A. Al-Laham, *ibid*. **94**, 6081 (1991).
[41] M. J. Frisch, G. W. Trucks, H. B. Schlegel, P. M. W. Gill, B. G. Johnson, M. A. Robb, J. R. Cheeseman, T. Keith, G. A. Petersson, J. A. Montgomery, K. Raghavachari, M. A. Al-Laham, V. G. Zakrzewski, J. V. Ortiz, J. B. Foresman, J. Cioslowski, B. B. Stefanov, A. Nanayakkara, M. Challacombe, C. Y. Peng, P. Y. Ayala, W. Chen, M. W. Wong, J. L. Andres, E. S. Replogle, R. Gomperts, R. L. Martin, D. J. Fox, J. S. Binkley, D. J. Defrees, J. Baker, J. P. Stewart, M. Head-Gordon, C. Gonzalez, and J. A. Pople, GAUSSIAN 94, Revision B.2, (Gaussian, Inc., Pittsburgh, PA, 1995).
[42] E. W.-G. Diau, S. C. Smith, C.-H. Hu, and H. F. Schaefer III (unpublished).
[43] (a) L. Fan and T. Ziegler, J. Am. Chem. Soc. **114**, 10 890 (1992); (b) T. Ziegler, Chem. Rev. **91**, 651 (1991).
[44] C. Sosa and C. Lee, J. Chem. Phys. **98**, 8004 (1993).
[45] (a) B. G. Johnson, C. A. Gonzales, P. M. W. Gill, and J. A. Pople, Chem. Phys. Lett. **221**, 100 (1994); (b) B. G. Johnson, P. M. W. Gill, and J. A. Pople, J. Chem. Phys. **98**, 5612 (1993); (c) P. M. W. Gill, B. G. Johnson, J. A. Pople, and M. J. Frisch, Chem. Phys. Lett. **197**, 499 (1992).
[46] (a) C. W. Murray, N. C. Handy, and R. D. Amos, J. Chem. Phys. **98**, 7145 (1993); (b) C. W. Murray, G. J. Laming, N. C. Handy, and R. D. Amos, Chem. Phys. Lett. **199**, 551 (1992).
[47] P. J. Stephens, F. J. Devlin, C. F. Chabalowski, and M. J. Frisch, J. Phys. Chem. **98**, 11623 (1994).
[48] G. Rauhut and P. Pulay, J. Phys. Chem. **99**, 3093 (1995).
[49] Y. Abashkin, N. Russo, E. Sicilia, and M. Toscano, in *Modern Density Functional Theory: A Tool for Chemistry*, edited by J. M. Seminario and P. Politzer (Elsevier, Amsterdam, 1995), Vol. 2, p. 255.
[50] J. Hrusak, H. Friedrichs, H. Schwarz, H. Razafinjanahary, and H. Chermette, J. Phys. Chem. **100**, 100 (1996).
[51] R. Neumann and N. C. Handy, Chem. Phys. Lett. **252**, 19 (1996).
[52] A. M. Lee and N. C. Handy, J. Chem. Soc. Faraday Trans. **89**, 3999 (1993).
[53] J. Baker, A. Scheiner, and J. Andzelm, Chem. Phys. Lett. **216**, 380 (1993).
[54] J. A. Pople, P. M. W. Gill, and N. C. Handy, Int. J. Quantum Chem. **56**, 303 (1995).
[55] J. F. Stanton, J. Chem. Phys. **101**, 371 (1994).
[56] W. Chen and H. B. Schlegel, J. Chem. Phys. **101**, 5957 (1994).
[57] L. A. Curtiss, D. L. Drapcho, and J. A. Pople, Chem. Phys. Lett. **103**, 437 (1984).
[58] (a) S. P. Walch, J. Chem. Phys. **98**, 1170 (1993); (b) S. P. Walch, R. J. Duchovic, and C. M. Rohlfing, *ibid*. **90**, 3230 (1989).
[59] S. F. Selgren, P. W. McLoughlin, and G. I. Gellene, J. Chem. Phys. **90**, 1624 (1989).
[60] E. W. Diau, A. M. Mebel, and M. C. Lin (unpublished result).
[61] D. L. Yang and J. L. Durant (unpublished result).
[62] E. W.-G. Diau, S. C. Smith, D. L. Yang, and J. L. Durant (unpublished).
[63] A similar check has also been done by $\Delta E(+)$=CCSD(T)/6-311+G(d,p)-CCSD(T)/6-311G(d,p), which gives -2.92 kcal mol^{-1} and -6.37 kcal mol^{-1} with respect to the reactants in comparison with the original G2M prediction, -3.48 kcal mol^{-1} and -10.06 kcal mol^{-1}, for TS *c* and TS *h*, respectively.
[64] L. A. Curtiss, J. E. Carpenter, and K. Raghavachari, J. Chem. Phys. **66**, 9030 (1992).